respectively. In the absence of CD_3OD (or CH_3OH) only **25** will be formed as is the case in the demethoxylations in CH_2Cl_2 and $CHCl_3$.

Subsequent fragmentation of **25** and **26** results in the formation of **17** (**18**) and **12** (1-OCH_3) and **22** (1-OCD_3 isomer), respectively.

It should be emphasized that data obtained by Solomon and Karlin and co-workers[2] on a phenoxo-bridged dinuclear peroxocopper(II) complex indicate either a nonsymmetrical μ-1,2-bridged peroxo ligand or a peroxo group bound to a single Cu(II) ion. It is not too far fetched to suggest that similar binding modes, shown schematically in Figure 1 (**27A** and **27B**), exist in complex **24** (CH_3CN omitted). Considering the next complex **28**, which is a *resonance structure* of **27A** and which can be formed from **27B** by copper–oxygen bond fission, it is conceivable that ipso attack of the peroxy group or deuteriomethanol can be a favorable pathway leading to **25** and **26**, respectively. Furthermore protonation of either **27A** or **27B** by methanol to form copper bound hydroperoxide and methoxide ion adjacent to the arene ring might contribute to the formation of **26**.[24] If **28** has an important contribution to the overall mechanism, it should be noted that this *formally* means an electron transfer from the arene ring to the peroxodicopper moiety.[25] Due to the presence of the imine bonds this does not likely lead to long-living arene-centered radicals, which is consistent with the high selectivity that is observed, although a one-electron oxidation by the peroxodicopper(II) group followed by highly selective radical type conversion cannot be excluded in the specific ligand system present here.

In conclusion the conversions of **4** and **8** represent, as far as we know, the first examples of an ipso hydroxylation induced demethoxylation of aryl ethers using copper ions and O_2.[26] Furthermore we provided evidence for competing pathways in aryl ether bond fissions and arene hydroxylations[5,6] by using copper monooxygenase model systems. Our data indicate that electrophilic attack[4a,5,22] on arenes, with formation of an arene peroxide bond in the first step, might not be an exclusive pathway for these model compounds. Further studies to support the proposed mechanisms are in progress.

Acknowledgment. We are grateful to Dr. H. E. Schoemaker for stimulating discussions and Mr. A. Kiewiet for mass spectral analyses.

(24) We acknowledge this suggestion made by one referee.
(25) Walling, C.; El-Taliawi, G. M.; Amarnath, K. *J. Am. Chem. Soc.* **1984**, *106*, 7573. Kersten, P. J.; Tien, M.; Kalyanaraman, B.; Kirk, T. N. *J. Biol. Chem.* **1985**, *260*, 2609. Nozaki, M. *Top. Curr. Chem.* **1979**, *78*, 145.
(26) See, also: Ito, S.; Kunai, A.; Okada, H.; Sasaki, K. *J. Org. Chem.* **1988**, *53*, 296.

Electron-Exchange Reactions between Heteropoly Anions: Comparison of Experimental Rate Constants with Theoretically Predicted Values†

Mariusz Kozik‡ and Louis C. W. Baker*

Contribution from the Department of Chemistry, Georgetown University, Washington, D.C. 20057. *Received May 15, 1989*

Abstract: This paper presents the first variable ionic strength study of the rates of intercomplex electron transfers between species wherein the electron to be exchanged is delocalized over numerous equivalent metal atoms. The complexes used were heteropoly tungstophosphates and their isomorphous heteropoly blue reduction products, the latter being class II mixed-valence species wherein the added "blue" electrons are delocalized over a dozen or more WO_6 units. Heteropoly complexes characteristically have extremely low interactions with solvent. Electron-exchange rates in solution were evaluated from ^{183}P NMR data. In the case of the nearly spherical α-$[PW_{12}O_{40}]^{3-}$ exchanging with its heteropoly blue 1e reduction product, the experimental rates coincide very closely with those calculated from current theory of electron transfer in solution. These results lead to the general conclusion that extensive electron delocalization (over all 12 WO_6 octahedra) does not significantly contribute to activation energy for intercomplex electron exchange. In the case of the paramagnetic 1e blue reduction product α-$[PW_{12}O_{40}]^{4-}$ exchanging with its diamagnetic 2e-reduced isomorph, there is intrusion of an energy consideration for unpairing the delocalized electron to be exchanged. This significantly lowers the electron-exchange rate. Other cases, wherein geometric factors are expected to lower the rates, gave deviations in the expected direction and in the expected order. The exchanging pairs considered are as follows: (1) α-$[PW_{12}O_{40}]^{3-}$ and its 1e heteropoly blue reduction product, (2) α-$[PW_{12}O_{40}]^{4-}$ and the corresponding 2e reduction product α-$[PW_{12}O_{40}]^{5-}$, (3) α-$[P_2W_{18}O_{62}]^{6-}$ and its 1e blue reduction product, and (4) α-$[PMo_3W_{15}O_{62}]^{6-}$ and its 1e blue reduction product.

Background

Reduced heteropoly anions constitute a large, distinct, and potentially important, group of mixed-valence complexes commonly known as "heteropoly blues".[1-3] Recently we reported the first NMR spectra of *paramagnetic* 1e-reduced heteropoly blues.[4] In 1e-reduced Mo-substituted derivatives of Wells–Dawson tungstophosphate anions,[5] α_1- and α_2-$[P_2MoW_{17}O_{62}]^{7-}$ (see Figure 1), the added electron is localized on the Mo,[3a,4] and the ^{31}P NMR signals of the phosphorus located nearer the reduced Mo atom are very broad ($\Delta\nu_{1/2}$'s of 900 and 400 Hz for the α_1 and α_2 isomers, respectively), as expected on the basis of their electronic ground states. On the other hand, in the complexes where the added electron is delocalized over part or all of a complex's

† Presented in part at the Third American Congress of the North American Continent, Toronto, June 1988, Inorganic Paper No. 204.
‡ Present address: Department of Chemistry, SUNY-Buffalo, Buffalo, NY 14214.

(1) Pope, M. T. *Heteropoly and Isopoly Oxometalates*; Springer-Verlag: Berlin, 1983; Chapter 6.
(2) Buckley, R. I.; Clark, R. J. H. *Coord. Chem. Rev.* **1985**, *65*, 167.
(3) (a) Kozik, M.; Hammer, C. F.; Baker, L. C. W. *J. Am. Chem. Soc.* **1986**, *108*, 2748. (b) Kozik, M.; Casañ-Pastor, N.; Hammer, C. F.; Baker, L. C. W. *Ibid.* **1988**, *110*, 7697. (c) Kozik, M.; Baker, L. C. W. *Ibid.* **1987**, *109*, 3159.
(4) Kozik, M.; Hammer, C. F.; Baker, L. C. W. *J. Am. Chem. Soc.* **1986**, *108*, 7627.
(5) (a) Wells, A. F. *Structural Inorganic Chemistry*, 1st ed.; Oxford University Press: Oxford, UK, 1945; p 344. (b) Dawson, B. *Acta Crystallogr.* **1953**, *6*, 113. (c) D'Amour, H. *Acta Crystallogr.* **1976**, *B32*, 729.

0002-7863/90/1512-7604$02.50/0

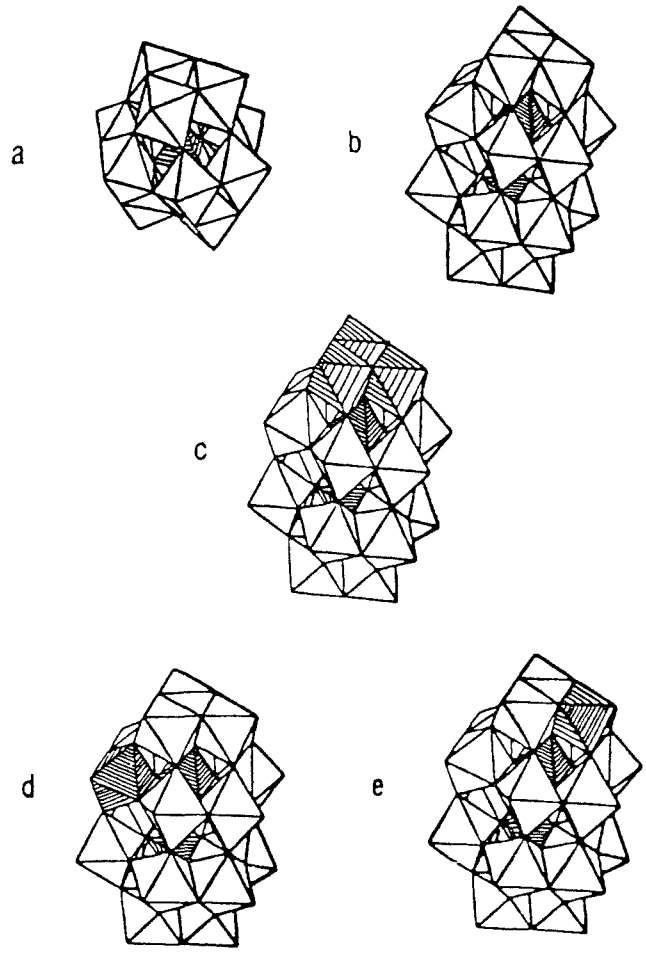

Figure 1. (a) Keggin structure of α-$[PW_{12}O_{40}]^{3-}$. (b) Wells–Dawson structure of α-$[P_2W_{18}O_{62}]^{6-}$. (c) Structure of α-$[P_2Mo_3W_{15}O_{62}]^{6-}$. (d) Structure of α_1-$[P_2MoW_{17}O_{62}]^{6-}$. (e) Structure of α_2-$[P_2MoW_{17}O_{62}]^{6-}$. Every vertex of a polyhedron locates the center of an oxygen atom. The P atoms are at the centers of the interior hatched tetrahedra. Within each white octahedron is a W atom, displaced significantly off-center toward the unshared oxygen atom of that octahedron. Each hatched octahedron contains a Mo atom similarly displaced toward the octahedron's unshared O. The exterior O atoms are heavily polarized toward the positive W or Mo atoms just beneath the exterior layer of O's, rendering H bonding to solvent minimal and causing hydrodynamic radii to correspond to the complexes' crystallographic radii.

structure, the ^{31}P NMR lines become much narrower. For example, the ^{31}P NMR signal from a 0.001 M solution of the 1e-reduced α Keggin[6] anion, α-$[PW_{12}O_{40}]^{4-}$, has a line width of only 1.7 Hz.

We have rationalized the narrowing of NMR line widths in those complexes that have one or more delocalized "blue" electrons by the decrease in the ^{31}P nuclear correlation time owing to the rapid thermal hopping of those electrons among the atoms over which they are delocalized. Comparison of the ^{31}P NMR line widths in complexes where the added electron is localized on a single Mo atom near the P, with the ^{31}P NMR line widths in isostructural complexes wherein the added electron is delocalized, enabled calculation[4] of the *intramolecular* electron hopping rates in α-$[P_2Mo_3W_{15}O_{62}]^{7-}$ and in α-$[P_2W_{18}O_{62}]^{7-}$.

We demonstrated[4] that ^{31}P NMR spectra can also be used to determine the *intermolecular* electron-exchange rates for heteropoly complexes. Thus, in equimolar mixtures of oxidized and reduced forms of the Wells–Dawson anion (α-$[P_2W_{18}O_{62}]^{6-/7-}$), the ^{31}P NMR lines broaden owing to the intercomplex electron-exchange process, the rate of which is in the intermediate-exchange/slow-exchange region of the NMR time scale.[7] In contrast, only one signal, centered exactly between the chemical shifts for the oxidized and reduced species, is observed for the equimolar mixtures of oxidized and 1e-reduced Keggin anions (α-$[PW_{12}O_{40}]^{3-/4-}$). This indicates a rate of intermolecular electron exchange in the intermediate-exchange/fast-exchange region of the NMR time scale. Comparison of the ^{31}P NMR line widths of 1e-reduced complexes with corresponding line widths in equimolar mixtures of oxidized and reduced anions led to calculation of intercomplex electron-exchange rates.

Our original publication[4] compared the experimental rate constants for the intercomplex electron exchange with the rates of diffusion and concluded that for both Keggin and Wells–Dawson tungstophosphates the electron-exchange rates approach the diffusion-controlled limit. Our calculations, however, did not consider the effect of ionic strength on the rates. In the present paper we extend the measurements to mixtures of α-$[PW_{12}O_{40}]^{3-}$ and α-$[PW_{12}O_{40}]^{4-}$ over the range of ionic strengths from 0.026 to 0.616. The experimentally determined rates are then seen to be much slower than the appropriate diffusion rates. However, the rates for the 1e-reduced versus oxidized Keggin species, wherein the distribution of the delocalized electron is essentially spherical, are in very good agreement with rates calculated theoretically on the basis of current semiclassical theory of outer-sphere electron transfer in solution. The agreement is excellent over the whole range of ionic strengths studied. This leads to the general conclusion that the electron delocalization of itself does not significantly contribute to the activation energy of intercomplex exchange in cases involving class II mixed-valence compounds having delocalization over numerous atoms.

Also reported herein are measurements of electron-exchange rates between the pair of complexes: paramagnetic 1e- and diamagnetic 2e-reduced Keggin tungstophosphates (α-$[PW_{12}O_{40}]^{4-/5-}$). For low ionic strengths the rate of electron exchange is in the intermediate-exchange/slow-exchange region of the NMR time scale, while for higher ionic strengths the rate reaches the intermediate-exchange/fast-exchange region. The experimentally determined rates are smaller than the rates calculated theoretically, owing, we suggest, to the additional activation energy required for the decoupling of the electron pair involved in the act of electron transfer.

The rates for (1) Wells–Dawson 18-tungstodiphosphate with its 1e reduction product and (2) the isomorphous 3-molybdo-15-tungstodiphosphate with its 1e reduction product are much slower than the rates predicted by theory of outer-sphere electron transfer. Geometrical considerations easily account for the disagreements and for the order of the rate decreases.

Experimental Section

All NMR spectra were recorded on an AM300 WB Bruker NMR spectrometer at 25 °C. Internal lock signal at 46.073 MHz was provided by the D_2O present in 20% concentration in all samples. The lithium salt of α-$[P_2W_{18}O_{62}]^{6-}$ and the free acid of α-$[PW_{12}O_{40}]^{3-}$ were reduced to 1e or 2e blues by constant potential electrolysis while the total of coulombs passed was monitored. Equimolar mixtures of oxidized and 1e-reduced, or of 1e- and 2e-reduced, complexes were prepared by Coulometrically monitored electrolytic reoxidation of each reduced species. Air was rigorously excluded at all times, and the NMR tubes were flame-sealed under argon.

Results and Discussion

For a mixture of oxidized and 1e-reduced Keggin α-12-tungstophosphate, a single broad peak centered exactly (±0.1 ppm) between the chemical shifts for the oxidized (−14.6 ppm) and 1e-reduced (−10.2 ppm) complexes was observed for six different ionic strengths. The line width of this peak decreases with increasing ionic strength. (See Table I). The spectra for the lowest (μ = 0.026) and the highest (μ = 0.616) ionic strengths are shown in Figure 2.

The ^{31}P NMR spectra of the equimolar mixture of 1e- and 2e-reduced blues of the Keggin complex changed significantly with ionic strength. There were, for each of the three lowest ionic

(6) (a) Keggin, J. F. *Proc. R. Soc.* **1934**, *A114*, 75. (b) Illingworth, J. W.; Keggin, J. F. *J. Chem. Soc.* **1935**, 575. (c) D'Amour, H.; Allmann, R. *Kristallogr. Z.* **1975**, 143, 1.

(7) Martin, M. L.; Martin, G. J.; Delpuech, J.-J. *Practical NMR Spectroscopy*; Heyden and Son: London, 1980.

Table I. ^{31}P Chemical Shifts, Line Widths, and Experimental Rate Constants for Electron-Exchange Reactions at Various Ionic Strengths (25 °C)

reactants	ionic strength	medium	^{31}P chemical shifts (ppm) (line widths at half-height (Hz))	rate constants,[a] M^{-1} s^{-1}
α-$[PW_{12}O_{40}]^{3-}$ and α-$[PW_{12}O_{40}]^{4-}$, each 1.0 mM (counterion H^+)	0.026	0.010 M HCl	−12.4 (82.0 ± 1.5)	(2.70 ± 0.16) × 10^6
	0.050	0.034 M HCl	−12.4 (38.0 ± 0.8)	(5.8 ± 0.4) × 10^6
	0.080	0.064 M HCl	−12.4 (22.0 ± 0.6)	(1.0 ± 0.8) × 10^7
	0.116	0.10 M HCl	−12.4 (19.0 ± 0.6)	(1.2 ± 0.1) × 10^7
	0.216	0.10 M HCl and 0.10 M NaCl	−12.4 (8.7 ± 0.2)	(2.8 ± 0.2) × 10^7
	0.616	0.10 M HCl and 0.50 M NaCl	−12.4 (3.5 ± 0.1)	(8.2 ± 0.8) × 10^7
α-$[PW_{12}O_{40}]^{4-}$ and α-$[PW_{12}O_{40}]^{5-}$, each 1.0 mM (counterion H^+)	0.050	0.025 M HCl	−10.2 (20.0 ± 0.6), −15.6 (20.0 ± 0.6)	(6.3 ± 0.2) × 10^4
	0.080	0.055 M HCl	−10.2 (46.0 ± 0.9), −15.6 (46.0 ± 0.9)	(1.4 ± 0.1) × 10^5
	0.125	0.10 M HCl	−10.2 (62.0 ± 1.2), −15.6 (62.0 ± 1.2)	(2.5 ± 0.1) × 10^5
	1.025	0.10 M HCl and 0.90 M NaCl	−12.9 (137.0 ± 2.5)	(2.5 ± 0.1) × 10^6
α-$[P_2W_{18}O_{62}]^{6-}$ and α-$[P_{12}W_{18}O_{62}]^{7-}$, each 0.010 M (counterion Li^+)	0.59	0.10 M HCl	−12.2 (4.5 ± 0.2), +0.2 (19.0 ± 0.5)	(1.1 ± 0.2) × 10^3
	1.49	0.10 M HCl and 0.90 M NaCl	−12.8 (46.5 ± 1.5), −0.4 (61.0 ± 2)	(1.1 ± 0.1) × 10^4

[a] Besides the uncertainties for $\Delta\nu_{1/2}$(mix), other sources of errors are uncertainties in $\Delta\nu_{1/2}$(1e), $\Delta\nu_{1/2}$(ox) (each taken as 0.1 Hz), and in p(le) and p(ox) (each taken as 0.005). Errors in M and $\Delta\nu$ (chemical shift difference, in hertz, between signals from pure ox species and pure le species) were found to contribute insignificantly to the errors in rate constants listed in Table I. Complete error analyses yielded the uncertainties listed for the rate constants in the table.

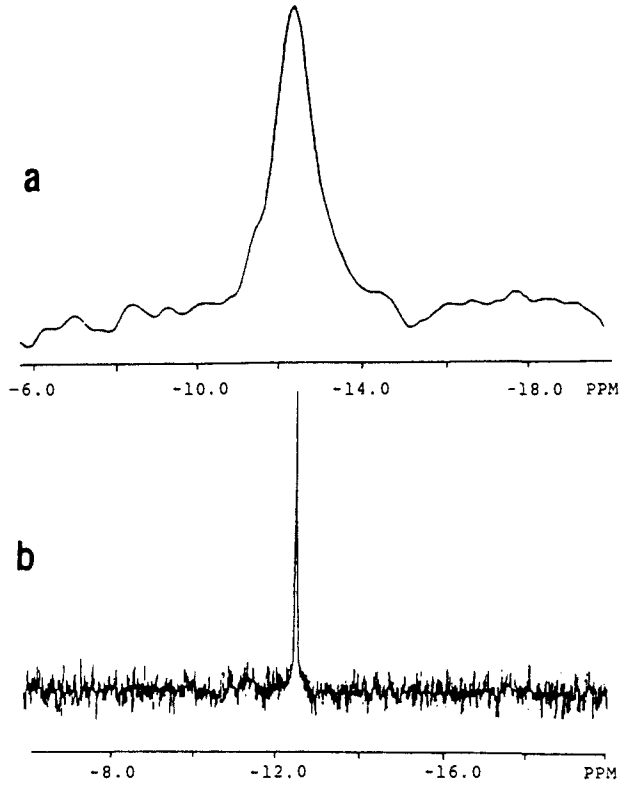

Figure 2. ^{31}P NMR spectra of mixtures containing 1.00 × 10^{-3} M α-$[PW_{12}O_{40}]^{3-}$ and 1.00 × 10^{-3} M α-$[PW_{12}O_{40}]^{4-}$ (1e blue). (a) Ionic strength 0.026, (0.010 M HCl), acquired through 13 984 scans over ~7 h. (b) Ionic strength 0.616 (0.10 M HCl, 0.50 M NaCl), acquired through 2000 scans over ~30 min.

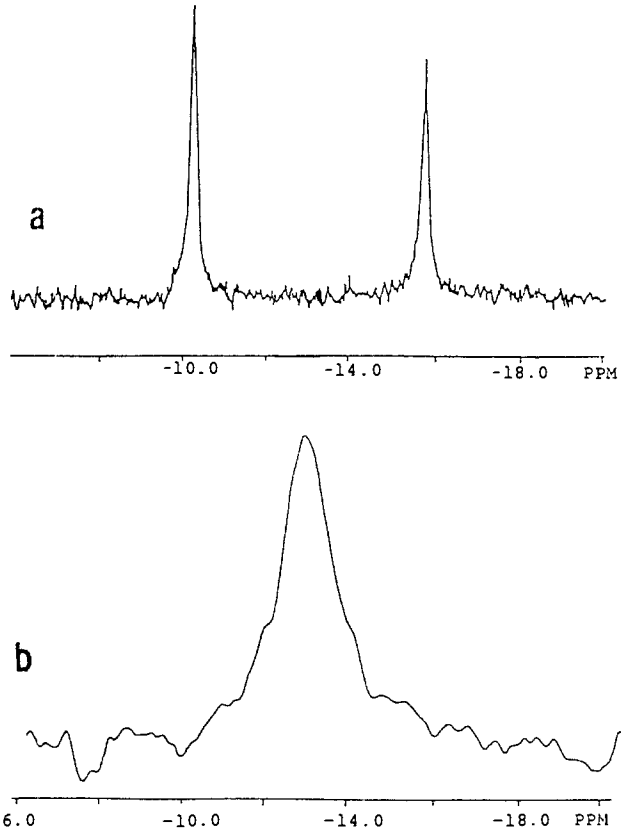

Figure 3. ^{31}P NMR spectra of mixtures containing 1.00 × 10^{-3} M α-$[PW_{12}O_{40}]^{4-}$ (1e blue) and 1.00 × 10^{-3} M α-$[PW_{12}O_{40}]^{5-}$ (2e blue). (a) Ionic strength 0.050, acquired through 9008 scans over ~2 h. (b) Ionic strength 1.025, acquired through 69 920 scans over ~20 h.

strengths, two peaks at the same chemical shifts as in solutions of pure 1e- and of pure 2e-reduced anions, but the line widths increased with increasing ionic strength. On the other hand at ionic strength μ = 1.025, only one signal, exactly halfway between the signals for the 1e- and 2e-reduced anions, was present ($\Delta\nu_{1/2}$ = 137 Hz). See Figure 3 for the spectra at ionic strengths 0.050 and 1.025.

For the equimolar mixture of oxidized and 1e-reduced Wells–Dawson complex (α-$[P_2W_{18}O_{62}]^{6-/7-}$), two ^{31}P peaks at the same chemical shifts as observed for pure nonreduced and pure 1e-reduced anions were observed. Both signals were broadened, in the mixture, relative to the signals in solutions of the pure nonreduced and the pure 1e-reduced anions. In the solution with ionic strength 0.59 (0.010 M nonreduced complex, 0.010 M 1e-reduced complex, and 0.10 M HCl), the signals were broadened by ~4 Hz, while in the solution with ionic strength 1.49 (the same concentrations of heteropoly anions as immediately above plus 0.10 M HCl + 0.90 M NaCl) both signals were broadened by ~46 Hz. See Figure 4 for both spectra. At smaller ionic strengths the changes of line widths were too small to be reliably measured.

The experiment was repeated for 2.0 mM total concentration of heteropoly complex. Only at a very high ionic strength (~1) could any changes in the line widths be measured reliably. In the solution with ionic strength 1.05 (1.0 mM nonreduced complex, 1.0 mM reduced complex, 0.10 M HCl, and 0.90 M NaCl), the line widths of both signals broadened by approximately 4 Hz.

The above-described spectra clearly indicate that intercomplex electron exchange takes place in the mixtures of oxidized and reduced heteropoly anions. The rate of electron exchange is in the intermediate/fast region of the NMR time scale for the case of oxidized and 1e-reduced α Keggin anion, and in the intermediate/slow region of the NMR time scale for the case of the oxidized and 1e-reduced α Wells–Dawson anion. The electron exchange between the 1e- and 2e-reduced α Keggin anions is in the intermediate/slow region for the three lowest ionic strengths measured, but it is in the intermediate/fast region for ionic strength μ = 1.025.

As we have indicated previously,[4] the electron-exchange process must be outer sphere and second order because oxygen exchange

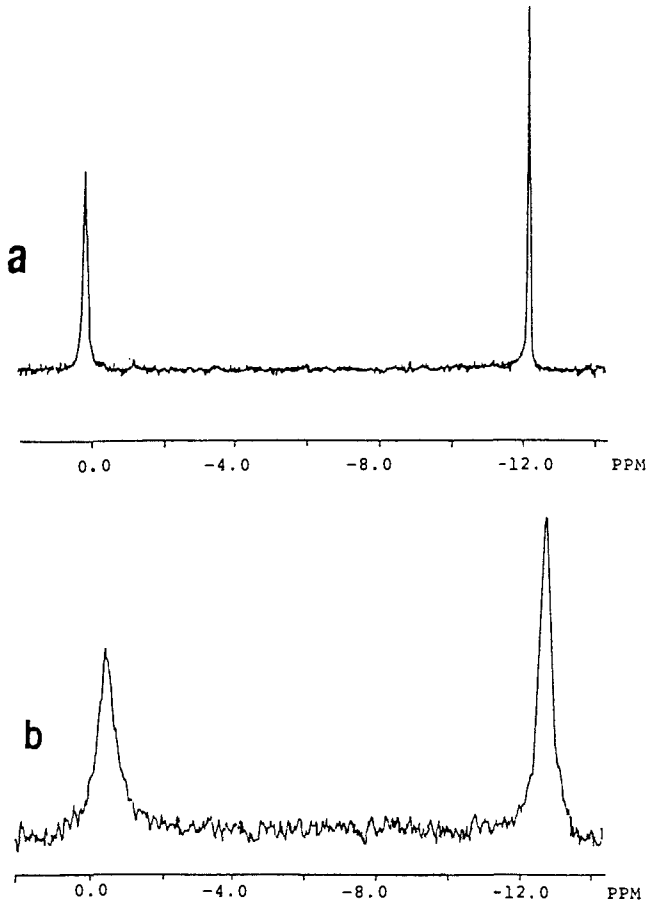

Figure 4. ^{31}P NMR spectra of mixtures containing 0.010 M α-$[P_2W_{18}O_{62}]^{6-}$ and 0.010 M α-$[P_2W_{18}O_{62}]^{7-}$ (1e blue). (a) Ionic strength 0.59 (0.10 M HCl), acquired through 48 scans. (b) Ionic strength 1.49 (0.10 M HCl, 0.90 M NaCl), acquired through 48 scans.

between solvent and these heteropoly species is very slow.[8] The electron-exchange lifetime, τ, for the case of intermediate/fast exchange in the mixtures of oxidized and 1e-reduced Keggin anion can be calculated[9] from eq 1, where $(\pi T_2)^{-1}$(mix) is $\Delta\nu_{1/2}$ (in hertz)

$$T_2^{-1}(\text{mix}) = p(1e)/T_2(1e) + p(\text{ox})/T_2(\text{ox}) + p^2(\text{ox})p^2(1e)(2\pi\Delta\nu)^2[\tau(1e) + \tau(\text{ox})] \quad (1)$$

for the ^{31}P peak in the mixture of oxidized and 1e-reduced anion; $(\pi T_2)^{-1}(1e)$ and $(\pi T_2)^{-1}(\text{ox})$ are $\Delta\nu_{1/2}$'s of the ^{31}P peaks for pure 1e-reduced and pure oxidized anion, respectively; $p(\text{ox})$ and $p(1e)$ are molar fractions of the anions in solution (and each $p = 0.5$ in the present cases); $\Delta\nu$ is the chemical shift difference (expressed in hertz) between the signals from the pure 1e-reduced species and the pure oxidized species, which is 524 Hz; and $\tau(1e) = \tau(\text{ox}) = \tau$(electron-exchange lifetime). The second-order rate constant for the electron-exchange process, k, relates to the electron-exchange lifetime by eq 2, where c is the total concentration of heteropoly species.

$$\tau^{-1} = kc \quad (2)$$

For the case of intermediate/slow exchange in the mixtures of oxidized and 1e-reduced Wells–Dawson anions

$$T_2^{-1}(\text{mix}) = T_2^{-1}(1e) + \tau^{-1} \quad (3)$$

where $(\pi T_2)^{-1}$(mix) is $\Delta\nu_{1/2}$ for the ^{31}P peak of the 1e heteropoly blue in the equimolar mixture, and

$$\tau^{-1} = k[\text{oxidized complex}] \quad (4)$$

For the mixtures of 1e- and 2e-reduced Keggin complexes, eqs 1 and 2 were used for the first three ionic strengths, and eqs 3 and 4 were used for the largest ionic strength. All experimentally determined rate constants are listed in Table I.

a. Pertinent Theoretical Approach. The complete current theory of electron-transfer (ET) reactions in solutions has been summarized and reviewed.[10] Only outer-sphere bimolecular electron-transfer reactions, i.e., reactions in which the reactants do not share a common atom or group, are pertinent here. The first step in such a reaction in solution is the diffusion together of the separated reactants to form a precursor complex. This is followed by electron transfer within the precursor complex to form a successor complex. Under these conditions the rate constant for the ET reaction, k, is given by[10]

$$k^{-1} = k_d^{-1} + k_{act}^{-1} \quad (5)$$

$$k_{act} = K_A(r)k_{el}(r) \quad (6)$$

$$K_A(r) = [(4\pi N_A r^2 \delta r)/1000] \exp[-w(r)/RT] \quad (7)$$

$$k_{el}(r) = \nu_n(r)\kappa_{el}(r)\kappa_n(r) \quad (8)$$

where k_d is the diffusion-controlled rate constant for the formation of the precursor complex from the separated reactants, k_{act} is the activation-controlled rate constant for the bimolecular reaction, $K_A(r)$ is the equilibrium constant for the formation of reactant pairs separated by a distance between r and $r + \delta r$, $w(r)$ is the work required to bring the reactants to the separation distance r, $\nu_n(r)$ is an effective nuclear frequency, $\kappa_n(r)$ is the nuclear factor, and $\kappa_{el}(r)$ is the electronic factor. The magnitudes of the nuclear and electronic factors range from zero to unity.

If the work to bring the reactants together is predominantly Coulombic, the reactants are spherical, and the radii of all the ions are equal ($a_1 = a_2 = a$), then[10e]

$$w(r) = z_1 z_2 e^2/D_s r[1 + \beta r(\mu)^{1/2}] \quad (9)$$

where $r = a_1 + a_2 = 2a$, z_1 and z_2 are the charges of the two reactants, D_s is the static dielectric constant of the medium, μ is ionic strength, and $\beta = (8\pi N_A e^2/1000 D_s k_B T)^{1/2}$.

Since internuclear distances and nuclear velocities do not change during an electronic transition (Franck–Condon principle), the actual electron transfer occurs at essentially constant nuclear configuration and momentum. This requirement is incorporated into classical electron-transfer theories by postulating that the electron transfer occurs at the intersection of the reactants' (precursor complex) and products' (successor complex) potential energy surfaces. The nuclear configuration changes involve both the inner and the outer (solvent) coordination shells of the reactants and products and are conveniently discussed in terms of the reorganization parameters λ_{out} and λ_{in}, which are calculated from the following equations:[10f]

$$\lambda_{out} = (\Delta e)^2(1/(2a_1) + 1/(2a_2) - 1/r)(1/n^2 - 1/D_s) \quad (10)$$

$$\lambda_{in} = (1/2)\sum f_i(d_1^\circ - d_2^\circ)_i^2 \quad (11)$$

In these expressions Δe is the charge transferred during the reaction, n is the refractive index of the medium, $f_i = 2f_1f_2(f_1 + f_2)$ is a reduced force constant for the ith inner-sphere vibration, $(d_1^\circ - d_2^\circ)_i$ is the corresponding difference in the equilibrium bond distances in the two oxidation states, and the summation is over all the intramolecular vibrations. In the high-temperature limit the reaction proceeds classically: the system acquires the nuclear configuration appropriate to the intersection region and the nuclear factor is given by[10f]

(8) (a) Spitsyn, V. I.; Aistova, R. I.: Vesil'ev, V. N. *Dokl. Akad. Nauk SSSR* **1955**, *104*, 741. (b) Fedotov, M. A.; Maksimouskeya, R. I.; Begalieva, D. U.; Il'yasova, A. K. *Izv. Akad. Nauk SSSR, Ser. Khim.* **1980**, *29*, 1025.

(9) Swift, T. J. In *NMR of Paramagnetic Molecules*; La Mar, G. N., Horrocks, W. deW., Jr., Holm, R. H., Eds.; Academic Press: New York, London, 1973; pp 60–65, 75.

(10) (a) Marcus, R. A. *Annu. Rev. Phys. Chem.* **1964**, *15*, 155. (b) Reynolds, W. L.; Lumry, R. W. *Mechanisms of Electron Transfer* Ronald Press: New York, 1966. (c) Marcus, R. A.; Sutin, N. *Biochim. Biophys. Acta* **1985**, *811*, 265. (d) Sutin, N. In *Inorganic Biochemistry*; Eichhorn, G. L., Ed.; Elsevier: New York, 1973; Vol. 2, p 611. (e) Sutin, N. *Acc. Chem. Res.* **1982**, *15*, 275. (f) Sutin, N. *Prog. Inorg. Chem.* **1983**, *30*, 441. (g) Cannon, R. D. *Electron Transfer Reactions*; Butterworths: London, 1980.

$$\kappa_n = \exp(-\Delta G^{\ddagger}/RT) \quad (12)$$

$$\Delta G^{\ddagger} = (\lambda/4)(1 + \Delta G^{\circ}_{AB}/\lambda)^2 \quad (13)$$

In the above expressions $\lambda = \lambda_{in} + \lambda_{out}$, and ΔG°_{AB} is the free-energy change for the reaction at separation distance r. ΔG°_{AB} is zero for an electron-exchange reaction.

In the classical model, ν_n is the frequency of passage across the barrier; that is, the frequency of the vibration that destroys the activated complex configuration. It is given by[10c-f]

$$\nu_n^2 = \sum \nu_i^2 E_i / \sum E_i \quad (14)$$

where $\nu_i = (f_i/\mu_i)^{1/2}/2\pi$ is the harmonic frequency of the ith mode (reduced mass μ_i) and $E_i/4$ is its contribution to the barrier. The value of ν_n ranges from $\sim 10^{12}$ to $\sim 10^{14}$ s^{-1}, depending on whether the barrier-crossing vibration is predominantly a solvent mode or a high-frequency intramolecular mode. It is often assumed,[11] however, to be equal to kT/h or $\sim 10^{13}$ s^{-1}.

The electronic factor of the reaction determines the probability that the electron transfer will occur in the intersection region. Within the Landau–Zener treatment of avoided crossings, the electronic factor is given by[10f,12]

$$\kappa_{el} + 2[1 - \exp(-\nu_{el}/2\nu_n)]/[2 - \exp(-\nu_{el}/2\nu_n)] \quad (15)$$

$$\nu_{el} = (2H_{AB}^2/h)(\pi^3/E_\lambda RT)^{1/2} \quad (16)$$

$$\nu_{el} = gH_{AB}^2/E_\lambda^{1/2}\ s^{-1} \quad (17)$$

where ν_{el} is an electronic frequency, E_λ is the energy of optical electron transfer, H_{AB} is the electronic coupling matrix element, and $g = 1.5 \times 10^{14}$ $kcal^{-3/2}$ s^{-1} at 25 °C.

For the diffusion-controlled reaction between two ions, where the potential energy is expressed by Coulomb's equation, the bimolecular rate constant at infinite dilution becomes[13]

$$k_{od} = z_1 z_2 N_A^2 D/\epsilon_0 \epsilon_r RT\ [\exp(z_1 z_2 N_A/4\pi\epsilon_0\epsilon_r rRT) - 1]^{-1} \quad (18)$$

where z_1 and z_2 are the charges of the ions, ϵ_r is the dielectric constant of the medium, ϵ_0 is the permittivity of vacuum, r is the hard-sphere collision distance, and D is the diffusion coefficient. At higher ionic strengths μ[13]

$$\log k_d = \log k_{od} + 2z_1 z_2 \alpha\sqrt{\mu}(1 + \beta r\sqrt{\mu}) \quad (19)$$

and the numerical values of α and β in water at 25 °C are $\alpha = 0.509$ and $\beta = 0.329 \times 10^8$ cm.

b. Calculation of Theoretically Predicted Rate Constants for the Electron-Exchange Reaction between α-$[PW_{12}O_{40}]^{3-}$ and α-$[PW_{12}O_{40}]^{4-}$ Complexes. (1) Diffusion-Controlled Rate Constant. The hydrodynamic radius for α Keggin ions was taken to be 5.6 Å,[6,14] and the diffusion coefficient of α-$[PW_{12}O_{40}]^{3-}$ has been found by polarography[14c] to be 4.4×10^{-10} m^2 s^{-1}. (This value has been corrected for a change in the medium.)[14d] Upon substitution of these values and all other constants into eq 18, the diffusion-controlled rate constant at infinite dilution, k_{od}, is calculated to be 1.3×10^7 M^{-1} s^{-1}. The values of k_d for different ionic strengths are then obtained from eq 19. They change from 2.2×10^8 M^{-1} s^{-1} (ionic strength 0.026) to 3.8×10^9 M^{-1} s^{-1} (ionic strength 0.616).

(2) Equilibrium Constant for the Formation of the Precursor Complex. Work Term. The work to bring the ions together is calculated from eq 9, where $z_1 = -3$, $z_2 = -4$, and $r = 11.2$ Å. It equals 4.54 kcal/mol for infinite dilution, and it changes from 2.85 kcal/mol for ionic strength 0.026 to 1.17 kcal/mol for ionic strength 0.616.

Preexponential Term. The preexponential term in eq 7 is calculated by taking r to be the center to center distance of two Keggin ions at the closest approach ($r = 11.2$ Å) and δr equal to 0.08 nm, as recently proposed by Sutin and Marcus.[10c] The calculated value of this term is 0.76.

Equilibrium Constant. Upon substitution of the values of the work term and preexponential terms into eq 7, $K_A(r)$ is found to be 3.4×10^{-4} M for zero ionic strength. It changes from 6.0×10^{-3} M for ionic strength 0.026 to 1.0×10^{-1} M for ionic strength 0.616.

(3) First-Order Rate Constant for Electron Exchange within the Precursor Complex. Frequency Factor. In the 1e-reduced Keggin complex, the electron is hopping among all W atoms, apparently through p orbitals of bridging oxygens.[1] It is assumed herein, on geometrical grounds, that the vibration most probably involved in activated complex formation and destruction is the $W-O_{ed}-W$ symmetric stretch, where O_{ed} denotes edge-sharing oxygens, which are exposed more toward the outside of the complex. The IR and Raman spectra of α Keggin and α Wells–Dawson anions have been reported and assigned.[15] The $W-O_{ed}-W$ vibration was found at 533 cm^{-1}, which gives 1.5×10^{13} s^{-1} for the frequency factor for the electron-transfer reaction.

Nuclear Factor. The solvent reorganization parameter, λ_{out}, is calculated from eq 10 to be 16.4 kcal/mol. Owing to the fact that the added electron occupies the nonbonding orbitals,[1] a contribution to the nuclear factor from λ_{in} is expected to be smaller than the contribution from λ_{out}. λ_{in} was calculated in the following manner. It is assumed that the only significant contribution to λ_{in} comes from the changes in W–O distances upon reduction. Only one WO_6 octahedron in each anion was taken into account since the electron transfer is from one octahedron in the reduced species to one in the oxidized species. The changes in W–O distances upon reduction were estimated on the basis of recently reported X-ray data for the oxidized and the 2e-reduced α Keggin 12-tungstocobaltates(II).[16a] In one WO_6 octahedron of a Keggin structure four types of W–O bonds exist: $W-O_{term}$, $W-O_{ctr}$, $W-O_{ed}$, and $W-O_{cor}$. In this notation O_{term} are terminal oxygens, each bonded only to one tungsten; O_{ctr} are the central oxygens, each bonded to the heteroatom and to three tungstens; O_{ed} oxygens are involved in edge sharing between adjacent WO_6 octahedra; and oxygens bridging tungstens through a corner are called O_{cor}.

Upon reduction of α-12-tungstocobaltate(II) by two electrons the following changes in the average W–O bond lengths are observed:[16a] $W-O_{term}$ decreased by 0.001 Å, $W-O_{ctr}$ increased by 0.035 Å, $W-O_{ed}$ decreased by 0.034 Å, and $W-O_{cor}$ increased by 0.065 Å. The corresponding changes after 1e reduction of α-12-tungstophosphate were assumed to be the same. No similar X-ray data exist for any 1e-reduced heteropoly anion, but recent X-ray structures[16b] for oxidized isopolydecatungstate and for two of its reduction products indicate changes of comparable magnitudes to those cited above in W–O distances when the oxidized species is first reduced but relatively negligible further change upon further reduction. This is as expected since the changes that facilitate intramolecular delocalization have already occurred as a result of the first reduction.

The slight changes in bond angles in the WO_6 octahedra have been ignored. If included they would increase λ_{in} slightly, acting toward a small improvement in the agreement between the calculated and experimental rate constants.

(11) Brown, G. M.; Sutin, N. *J. Am. Chem. Soc.* **1979**, *101*, 883.
(12) Sutin, N.; Brunschwig, B. S. *ACS Symp. Ser.* **1982**, No. 198, 105.
(13) Moore, J. W.; Pearson, R. G. *Kinetics and Mechanisms*, 3rd ed.; John Wiley and Sons: New York, 1981; pp 260–276.
(14) (a) Baker, M. C.; Lyons, P. A.; Singer, S. J. *J. Am. Chem. Soc.* **1955**, *77*, 2011. (b) Kurucsev, T.; Sargeson, A. M.; West, B. O. *J. Phys. Chem.* **1957**, *61*, 1569. (c) Pope, M. T.; Varga, G. M., Jr. *Inorg. Chem.* **1966**, *5*, 1249. (d) Pope, M. T.; Papaconstantinou, E. *Inorg. Chem.* **1967**, *6*, 1147. (e) The D values given in refs 14c and 14d were determined for α-$[PW_{12}O_{40}]^{3-}$ in 1.0 M H_2SO_4 and for α-$[P_2W_{18}O_{62}]^{6-}$ in a solution simultaneously 0.10 M in H_2SO_4 and 0.9 M in Na_2SO_4. The data in the present paper were taken in the solutions listed in Table I. Since $D = kT/6\pi\eta r$, the D values were corrected for the changes in viscosities as listed in standard handbooks. The corrections of the D's affect only the values of k_d and therefore have little influence on the final values of k.
(15) (a) Rocchiccioli-Deltcheff, C.; Thouvenot, R.; Fouassier, M. *Inorg. Chem.* **1982**, *21*, 30. (b) Rocchiccioli-Deltcheff, C.; Fournier, M.; Franck, R.; Thouvenot, R. *Inorg. Chem.* **1983**, *22*, 207. (c) Thouvenot, R.; Fournier, M.; Franck, R.; Rocchiccioli-Deltcheff, C. *Inorg. Chem.* **1984**, *23*, 598.
(16) (a) Calculated from X-ray data reported in Casañ-Pastor, N. Doctoral Dissertation, Georgetown University, 1988. (b) Sasaki, Y.; Yamase, T.; Ohashi, Y.; Sasada, Y. *Bull. Chem. Soc. Jpn.* **1987**, *60*, 4285.

Table II. Calculated (k_d, k_{act}, and k) and Experimentally Observed (k_{exp}) Rate Constants (M^{-1} s^{-1}) at Various Ionic Strengths for the Electron-Exchange Reactions (1) between α-$[PW_{12}O_{40}]^{3-}$ Anion and Its 1e Blue and (2) between α-$[PW_{12}O_{40}]^{4-}$ (1e blue) and α-$[PW_{12}O_{40}]^{5-}$ (2e blue) (25 °C)

reactants	ionic strength	k_d[a]	k_{act}[a]	k[a]	k_{exp}[b]
α-$[PW_{12}O_{40}]^{3-}$/α-$[PW_{12}O_{40}]^{4-}$	0.0	1.3×10^7	3.7×10^5	3.6×10^5	$(1.1 \pm 0.2) \times 10^5$[c]
	0.026	2.2×10^8	6.6×10^6	6.4×10^6	2.7×10^6
	0.050	4.1×10^8	1.2×10^7	1.2×10^7	5.8×10^6
	0.080	6.5×10^8	2.0×10^7	1.9×10^7	1.0×10^7
	0.116	9.1×10^8	2.8×10^7	2.7×10^7	1.2×10^7
	0.216	1.6×10^9	5.0×10^7	4.8×10^7	2.8×10^7
	0.616	3.8×10^9	1.1×10^8	1.0×10^8	8.2×10^7
α-$[PW_{12}O_{40}]^{4-}$/α-$[PW_{12}O_{40}]^{5-}$	0.0	1.2×10^5	2.2×10^3	2.2×10^3	$(1.6 \pm 0.3) \times 10^2$[c]
	0.050	3.9×10^7	7.4×10^5	7.3×10^5	6.3×10^4
	0.080	8.2×10^7	1.5×10^6	1.5×10^6	1.4×10^5
	0.125	1.7×10^8	3.2×10^6	3.1×10^6	2.5×10^5
	1.025	2.8×10^9	5.5×10^7	5.4×10^7	2.5×10^6

[a] The uncertainties in all the calculated rate constants are indicated by the numbers of significant figures shown. [b] The experimentally determined values for rate constants have the uncertainties listed in Table I. [c] Obtained by extrapolation.

Complete normal-coordinate analysis of the IR spectra for polyoxometallates have been reported to date only for isopoly hexamolybdate and hexatungstate.[15a,17] This isopolyanion structure has two of the types of oxygens discussed for the α Keggin species (O_{term}, and O_{ed}). It lacks corner-sharing oxygens. Three stretching force constants were identified for the hexatungstate: k_{ctr} (0.84 mdyn/Å), k_{term} (8.30 mdyn/Å), and k_{ed} (2.80 mdyn/Å). These values of force constants are assumed for the W–O_{term} and W–O_{ed} stretching vibrations in both the α-tungstophosphate and its 1e blue. The force constant for the vibration responsible for stretching of the W–O_{cor} bond in the Keggin structure was estimated by Kazanskii[18] to be 4.1 mdyn/Å. It will be noted that the force constant for W–O_{ctr} stretching in the hexatungstate is by far the smallest of all the force constants cited. This results from the long W–O_{ctr} distances caused by each W being far off-center in its WO_6 octahedron, close to its O_{term} atom. Although each interior (O_{ctr}) oxygen atom in α-$[PW_{12}O_{40}]^{3-}$ has three W's and one P for nearest neighbors while the O_{ctr} in hexatungstate has six nearest W neighbors, the O_{ctr}–W distance in the heteropoly complex is also very long for the same reason as pertains in hexatungstate. Its stretching force constant will therefore also be low, and use of any low value in the neighborhood of k_{ctr} = 0.84 mdyn/Å will yield essentially the same result for λ_{in} when all the data are substituted into eq 11. Such substitution gives λ_{in} = 6.1 kcal/mol for the inner-sphere contribution to the nuclear factor. The relatively small contribution of λ_{in} to the nuclear factor indicates that inaccuracies in the assumptions, bond lengths, or force constants cited above would not introduce large errors in the k finally predicted.

The nuclear factor is calculated by using eq 12, and taking into account the fact that $\Delta G°$ is zero for any electron-exchange reaction. Its value is 8.0×10^{-5} at 25 °C.

Electronic Factor. In order to calculate κ_{el}, a numerical value of H_{AB} (electronic coupling matrix) has to be estimated. The distance dependence of H_{AB} can be approximated by[10c]

$$H_{AB} = H^{o}_{AB} \exp[-b(r - \sigma)] \qquad (20)$$

where H^{o}_{AB} is the value of H_{AB} when $r = \sigma$.[10c,19] Values of H_{AB} for intramolecular electron transfer in several heteropoly tungstates were reported by Sanchez et al.[20] H_{AB} has a value of 0.31 eV (7.14 kcal/mol) in α Keggin tungstosilicate anion,[20a] where the average W–W distance is 3.6 Å.[21] In 1982, Sanchez et al.[20b] estimated from ESR line widths that b = 10–13 nm^{-1} for α-$[PMo_{12}O_{40}]^{4-}$. In the present work, b was taken as 12 nm^{-1}, which is the currently accepted value[10c,19] for nonbiological systems. The closest W–W approach (as it is in α Keggin tungstophosphate[22]) in intermolecular electron exchange is estimated (from three-dimensional models of α Keggin ions) to be ~5.1 Å. This yields H_{AB} equal to 1.2 kcal/mol. The wavelength of the intervalence charge-transfer transition for the 1e blue of α-$[PW_{12}O_{40}]^{3-}$ complex has been reported by Varga et al.[23] (E_λ = 22.9 kcal/mol). Upon substituting these values of H_{AB} and E_λ into eq 17 one gets ν_{el} = 4.6×10^{13} s^{-1} and the electronic factor (from eq 15) equals 0.90.

The product of frequency, electronic, and nuclear factors is $k_{el}(r)$ = 1.1×10^9 s^{-1}.

(4) Activation-Controlled Rate Constant. The bimolecular activation-controlled rate constant was calculated from eq 6. For infinite dilution it has a value of 3.7×10^5 M^{-1} s^{-1}. It changes from 6.6×10^6 M^{-1} s^{-1} for ionic strength 0.026 to 1.1×10^8 M^{-1} s^{-1} for ionic strength 0.616.

(5) Bimolecular Rate Constant for Electron-Exchange Reaction. The final theoretically predicted rate constant for electron exchange between the oxidized complex and its 1e reduction product was calculated from eq 5. It changes from 3.6×10^5 M^{-1} s^{-1} for zero ionic strength to 1.0×10^8 M^{-1} s^{-1} for ionic strength 0.616.

Theoretically predicted rate constants for the electron exchange between 1e- and 2e-reduced α Keggin complexes were calculated by using the same parameters as for the electron exchange between oxidized and 1e-reduced complexes, changing only the charges of the species involved (−4 and −5).[24] The values thus calculated change from 2.2×10^3 M^{-1} s^{-1} for zero ionic strength to 5.4×10^7 M^{-1} s^{-1} for ionic strength 1.025. See Table II.

c. Comparison of the Calculated and Experimentally Determined Rate Constants for Electron Exchange between Heteropoly Complexes. To our knowledge the data presented herein are the first variable ionic strength measurements of intercomplex electron exchange between class II mixed-valence metal complexes in solutions. Although much research has been reported in the area of intramolecular electron exchange between different metal centers in mixed-valence compounds[25] and intermolecular electron transfer between mononuclear complexes,[10] no data have been

(17) Rocchiccioli-Deltcheff, C.; Fournier, M.; Franck, R.; Thouvenot, R. *J. Mol. Struct.* **1984**, *114*, 49.

(18) Kazanskii, L. P. *Bull. Acad. Sci. USSR, Div. Chem. Sci. (Engl. Transl.)* **1975**, 432; *Izvest. Akad. Nauk SSSR, Ser. Khim.* **1975**, 502.

(19) Miller, J. R.; Beitz, J. V.; Huddleston, R. K. *J. Am. Chem. Soc.* **1984**, *106*, 5057.

(20) (a) Sanchez, C.; Livage, J.; Launay, J. P.; Fournier, M. *J. Am. Chem. Soc.* **1983**, *105*, 6817. (b) Sanchez, C.; Livage, J.; Launay, J. P.; Fournier, M.; Jeanin, Y. *J. Am. Chem. Soc.* **1982**, *104*, 3194. (c) H_{AB} values in refs 20a and 20b were estimated by using the equation $E_{th} = {}^1/_4E_{op} - H_{AB} + H^2_{AB}/E_{op}$, where E_{op} is the energy of the intervalence transition and E_{th} is the thermal activation energy for *intra*molecular electron hopping. E_{th} was estimated from the variation of ESR line widths with temperature.

(21) Smith, P. M. Doctoral Dissertation, Georgetown University, 1971; *Diss. Abstr.* **1972**, *B32*, 5136.

(22) Brown, G. M.; Noe-Spirlet, M. R.; Busing, W. R.; Levy, H. A. *Acta Crystallogr.* **1977**, *B33*, 1038.

(23) Varga, G. M., Jr.; Papaconstantinou, E.; Pope, M. T. *Inorg. Chem.* **1970**, *9*, 662.

(24) Lack of sufficient data about changes of W–O bond lengths upon further reduction of 1e-reduced species introduces uncertainties about the size of λ_{in} for this exchange. Since λ_{in} is relatively small in any case, the same value (λ_{in} = 6.1 kcal/mol) was assumed as calculated for the previous exchange. If λ_{in} were even as low as zero, the theoretically predicted values of k would increase by only 1 order of magnitude, increasing the theoretically predicted electron-exchange rate.

(25) Meyer, T. J. In *NATO Advanced Study Institute Series, Ser. C* Brown, D. B., Ed.; D. Reidel Publishing Co.: Dordrecht, The Netherlands, 1980, pp 73–113.

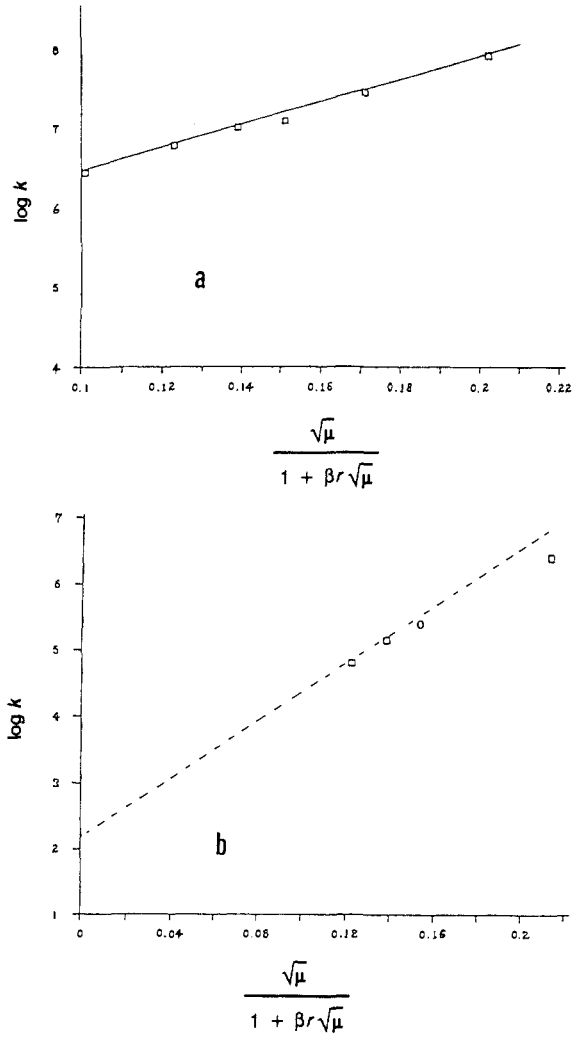

Figure 5. (a) Plot of log k versus $\mu^{1/2}/[1 + \beta r(\mu)^{1/2}]$ for the electron-exchange reaction between α-$[PW_{12}O_{40}]^{3-}$ and α-$[PW_{12}O_{40}]^{4-}$ (1e blue). The line shows the experimental slope. (b) Plot of log k versus $\mu^{1/2}/[1 + \beta r(\mu)^{1/2}]$ for the electron-exchange reaction between α-$[PW_{12}O_{40}]^{4-}$ (1e blue) and α-$[PW_{12}O_{40}]^{5-}$ (2e blue). The dashed line shows the slope predicted theoretically by the Debye-Hückel equation.

reported heretofore for intermolecular electron transfer for the case where the exchanging electron is delocalized over several metal centers in the participating complexes.

The experimental rate constants for the electron exchange between oxidized and 1e-reduced α Keggin complexes were fitted to the Debye-Hückel equation

$$\log k = \log k_0 + 2z_1z_2\alpha\sqrt{\mu}/(1 + \beta r\sqrt{\mu}) \qquad (21)$$

A plot of log k vs $\mu^{1/2}/(1 + \beta r(\mu)^{1/2}$ (r = 11.2 Å) is shown in Figure 5. Least-squares analysis of the data shows that the plot is a straight line with a slope of 14.5 and a correlation coefficient of 0.998. The theoretically predicted slope is 12.3. The results show that the Debye-Hückel equation quite adequately accounts for the ionic strength dependence of the rate constant even at rather unexpectedly high ionic strengths (>0.500 M), even though the equation was originally derived only for ionic concentrations smaller than 0.01 M. This may be explained by the fact that heteropoly anions, owing to the very pronounced inward polarization of their exterior oxygen atoms, have extremely low solvation energies and very low van der Waals attractions for one another.[26]

Table II combines the calculated (k_d, k_{act}, and k) and experimentally observed rate constants (k_{exp}) for different ionic strengths for the electron exchange between oxidized and 1e-reduced α Keggin anions. The calculated bimolecular rate constants (k's) are in good agreement with the experimentally observed values. This result indicates that the theoretical equations for rate constants of electron-transfer reactions in solutions, commonly used for monocenter complexes, can also be applied to the case where the exchanging electron is unpaired and delocalized over several metal centers in the participating complexes (in this case 12 centers).

Also shown in Table II are the calculated and experimentally determined rate constants for exchanges between 1e and 2e blues of the same α Keggin complex at different ionic strengths. The Debye-Hückel plot of the experimentally determined rate constants is shown in Figure 5b. A small deviation from linearity is seen at ionic strengths greater than 1. This is not surprising in view of the progressively increasing failure of Debye-Hückel theory to fit activity coefficients at high ionic strengths.[11,27] The data do have, however, the correct Debye-Hückel limiting slope of ~21 (dashed line in Figure 5b). For the first three points, which follow the Debye-Hückel equation well, the experimentally determined rate constant is 10-15 times smaller than the rate constant predicted theoretically. This difference presumably reflects the additional energy needed to decouple the paired electrons (in the 2e blue) so that one of them can be exchanged. In the 2e heteropoly blues, the added electrons are completely paired by multiroute superexchange although those electrons are always relatively widely separated, being on different atoms. Therefore, the Coulombic repulsions between them, which primarily account for the endothermic nature of electron pairing in a single atom, are virtually absent, and it is the unpairing process that is endothermic in a heteropoly blue.

The theoretically predicted rate constants for electron exchange between α-$[P_2W_{18}O_{62}]^{6-}$ and its 1e blue were calculated for different ionic strengths by following the same procedure used for the case of α Keggin complexes and using a hydrodynamic radius, a, of 6.4 Å,[28] charges of anions -6 and-7, and diffusion coefficient $D = 2.0 \times 10^{-10}$ M^{-1} s^{-1}.[29] The calculated rate constant for infinite dilution is 1.5×10^{-1} M^{-1} s^{-1}, and it changes from 9.9×10^6 M^{-1} s^{-1} for ionic strength 0.59 to 5.5×10^7 M^{-1} s^{-1} for ionic strength 1.49. The experimentally observed rate constants are 1.1×10^3 M^{-1} s^{-1} for ionic strength 0.59 and 1.4×10^4 M^{-1} s^{-1} for ionic strength 1.49. (Rates at ionic strengths lower than 0.49 were too slow to be determined from the changes in line widths.) It is evident that the observed rate constants are approximately 3 orders of magnitude lower than the theoretically predicted values. At least two different reasons may be suggested to explain this big difference. First, the Wells-Dawson complex is not essentially spherical as are the Keggin complexes. Its actual shape is an elongated ellipsoid (Figure 1), while the calculations were based on the assumption of a spherical shape. This fact itself could not, however, account for 3 orders of magnitude difference between the experimental and calculated values. Second, the charge distribution in the 1e blue of the Wells-Dawson anion is not expected to be uniform, because of both the nonspherical shape and the fact that the added "blue" electron is essentially delocalized only over the 12 "belt" W atoms of the complex.[3a,20] This effect must significantly increase the charge density on the belts of the reduced complexes. Simultaneously, the delocalization of the "blue" electron over only belt W atoms adds large geometrical constraints on orientation of the 18-tungstodiphosphate complexes during the process of electron exchange.

(26) (a) Baker, L. C. W.; Lebioda, L.; Grochowski, J.; Mukherjee, H. G. *J. Am. Chem. Soc.* **1980**, *102*, 3274. (b) Baker, L. C. W.; Pope, M. T. *J. Am. Chem. Soc.* **1960**, *82*, 4176. (c) Pope, M. T.; Baker, L. C. W. *J. Phys. Chem.* **1959**, *63*, 2083. (d) Yannoni, N. F. Doctoral Dissertation, Boston University, 1961; *Diss. Abstr.* **1961**, *22*, 1032.

(27) Robinson, R. A.; Stokes, R. H. *Electrolyte Solutions*, 2nd ed.; Academic Press: New York, 1959; p 227.

(28) Harmalker, S. P. Doctoral Dissertation, Georgetown University, 1982. The hydrodynamic radius of the Wells-Dawson structure is taken as 6.4 Å in accordance with Harmalker's determination from reorientational correlation times based on ESR line widths at various temperatures, using the Wells-Dawson isomorph α-$[P_2W_{17}VO_{62}]^{8-}$. This hydrodynamic radius supersedes the one quoted in ref 4.

(29) Pope, M. T.; Papaconstantinou, E. *Inorg. Chem.* **1967**, *6*, 1147.

Apparently it is similar factors that make the rate of electron exchange between α-$[P_2Mo_3W_{15}O_{62}]^{6-}$ and α-$[P_2Mo_3W_{15}O_{62}]^{7-}$ even slower than between 18-tungsto complexes.[4] In the 1e blue of α-$[P_2Mo_3W_{15}O_{62}]^{6-}$ the added electron is delocalized only over the three Mo atoms in one cap of the complex.[3a] This probably necessitates Mo cap to Mo cap contact during an electron exchange (which is much less probable than belt to belt contact) and significantly increases the charge density in the 3 Mo cap (again more than the analogous process in the α-$[P_2W_{18}O_{62}]^{6-}$ anion).

Acknowledgment. This research was supported in part by NSF Grant CHE-8406088 and by an instrument grant from the W. M. Keck Foundation.

Registry No. α-$[PW_{12}O_{40}]^{3-}$, 12534-77-9; α-$[PW_{12}O_{40}]^{4-}$, 12534-78-0; α-$[P_2W_{18}O_{62}]^{6-}$, 90751-95-4; α-$[P_2Mo_3W_{15}O_{62}]^{6-}$, 89173-94-4.

Models for Iron-Oxo Proteins. Mössbauer and EPR Study of an Antiferromagnetically Coupled $Fe^{III}Ni^{II}$ Complex

T. R. Holman,[†] C. Juarez-Garcia,[‡] M. P. Hendrich,[‡] L. Que, Jr.,*[,†] and E. Münck*[,‡]

Contribution from the Department of Chemistry, University of Minnesota, Minneapolis, Minnesota 55455, and Gray Freshwater Biological Institute, P.O. Box 100, County Roads 15 and 19, Navarre, Minnesota 55392. *Received February 21, 1990*

Abstract: The bimetallic complex $[Fe^{III}Ni^{II}BPMP(OPr)_2](BPh_4)_2$, where BPMP is the anion of 2,6-bis[(bis(2-pyridylmethyl)amino]methyl]-4-methylphenol, has been synthesized and its structure determined by X-ray diffraction methods as having a (μ-phenoxo)bis(μ-carboxylato) core. The complex crystallizes in the triclinic space group $P\bar{1}$ with cell constants: a = 13.607 (3) Å, b = 13.700 (3) Å, c = 25.251 (7) Å, α = 77.29 (2)°, β = 78.25 (2)°, γ = 61.73 (2)°, Z = 2, V = 4017 (4) Å^3. The metal centers have distinct six-coordinate N_3O_3 environments and are separated by 3.378 (8) Å, similar to related complexes in this series. We have studied the complex with EPR and Mössbauer spectroscopy and magnetic susceptibility. All three techniques establish that the electronic ground state of the complex has spin S = 3/2. For T < 10 K the EPR spectra are dominated by signals of the S = 3/2 multiplet. At higher temperatures, an additional resonance appears. It is centered at g = 4.2 and belongs to an excited multiplet with S = 5/2. We have studied the low-temperature Mössbauer spectra of the complex in external fields up to 6.0 T. Analysis of the well-resolved spectra yields D = 0.7 cm^{-1} and E/D = 0.32 for the zero-field splitting parameters of the S = 3/2 multiplet. Spectra taken in external fields H < 0.5 T reveal that D and E/D are distributed; a simple Gaussian distribution of E/D values fits the data quite well. The Mössbauer spectra show that the Fe^{III} site is high-spin. It follows that the dinuclear complex consists of a ferric ion (S_1 = 5/2) which is antiferromagnetically coupled to a high-spin (S_2 = 1) Ni^{II}. Analysis of the temperature dependence of the g = 4.2 EPR signal yields J = +24 (3) cm^{-1} ($\mathcal{H} = J\mathbf{S}_1\cdot\mathbf{S}_2$); the susceptibility study agrees with this result. Analysis of the ^{57}Fe magnetic hyperfine interaction with a spin coupling model yields A = -29.6 (2) MHz; this compares well with $A(Fe^{III})$ = -29.5(2) MHz which we obtained here for the Fe^{III} site of the isostructural $Fe^{III}Zn^{II}$ complex.

The study of metal-metal interactions has been an area of fascination for chemists and physicists, because of their potential impact in materials science, catalysis, and metallobiochemistry. The ubiquitous participation of metal sites involving more than one metal center in metalloproteins has heightened the interest of bioinorganic chemists in such interactions. Antiferromagnetic exchange coupling is a prominent feature of the magnetic properties of dicopper sites in hemocyanin, tyrosinase, and laccase[1-3] and diferric sites in plant-type ferredoxins,[4] methemerythrin,[5,6] and ribonucleotide reductase.[7] More recently, double exchange has been used to describe the properties of polyiron centers in ferredoxin II from *Desulfovibrio gigas* and the high potential iron protein.[8] In all these examples the metal-metal interaction represents the dominant factor that determines the spin physics of the metal site, with the zero-field splitting of the individual metal centers (if present) acting as a small perturbation on the spin coupled levels. However, examples of dinuclear sites are emerging wherein the exchange interaction is comparable in magnitude to the zero-field splitting. This is a result of the recent increased focus on the mixed valence and diferrous states of the dinuclear iron-oxo proteins. For example, the dramatic broadening of the EPR signals of the purple acid phosphatase from porcine uterus (uteroferrin) upon phosphate binding is ascribed to such an interplay between antiferromagnetic exchange and zero-field splitting.[9] The integer spin EPR signals observed for the diferrous forms of hemerythrin,[10] ribonucleotide reductase,[11] and methane monooxygenase[12] need to be evaluated in this context as well.

In an effort to understand such systems, we have embarked on combined EPR, Mössbauer, and magnetic susceptibility studies of dinuclear complexes with the goal of describing all the spectroscopic and magnetic properties with a consistent set of parameters. We have taken advantage of our ability to systematically generate heterobimetallic complexes to provide model systems for

[†] University of Minnesota.
[‡] Gray Freshwater Biological Institute.

(1) Solomon, E. I. In *Metal Clusters in Proteins*; Que, L., Jr., Ed.; American Chemical Society: Washington, DC, 1988; pp 116-152.
(2) Solomon, E. I.; Dooley, D. M.; Wang, R. H.; Gray, H. B.; Cerdonio, M.; Mogno, F.; Romani, G. L. *J. Am. Chem. Soc.* **1976**, *98*, 1029-1031.
(3) Petersson, L.; Angstrom, J.; Ehrenberg, A. *Biochim. Biophys. Acta* **1978**, *526*, 311-317.
(4) Sands, R. H.; Dunham, W. R. *Quart. Rev. Biophys.* **1975**, *4*, 443-504.
(5) Dawson, J. W.; Gray, H. B.; Hoenig, H. E.; Rossman, G. R.; Schreder, J. M.; Wang, R. H. *Biochemistry* **1972**, *11*, 461-465.
(6) Maroney, M. J.; Kurtz, D. M., Jr.; Nocek, J. M.; Pearce, L. L.; Que, L., Jr. *J. Am. Chem. Soc.* **1986**, *108*, 6871-6879.
(7) Petersson, L.; Graslund, A.; Ehrenberg, A.; Sjoberg, B.-M.; Reichard, P. *J. Biol. Chem.* **1980**, *255*, 6706-6712.
(8) (a) Papaefthymiou, V.; Girerd, J. J.; Moura, I.; Moura, J. J. G.; Münck, E. *J. Am. Chem. Soc.* **1987**, *109*, 4703-4710. (b) Noodleman, L. *Inorg. Chem.* **1988**, *27*, 3677-3679.
(9) Day, E. P.; David, S. S.; Peterson, J.; Dunham, W. R.; Bonvoisin, J. J.; Sands, R. H.; Que, L., Jr. *J. Biol. Chem.* **1988**, *263*, 15561-15567.
(10) Reem, R. C.; Solomon, E. I. *J. Am. Chem. Soc.* **1987**, *109*, 1216-1226.
(11) Lynch, J. B.; Juarez-Garcia, C.; Münck, E.; Que, L., Jr. *J. Biol. Chem.* **1989**, *264*, 8091-8096.
(12) Fox, B. G.; Surerus, K. K.; Münck, E.; Lipscomb, J. D. *J. Biol. Chem.* **1988**, *263*, 10553-10556.

0002-7863/90/1512-7611$02.50/0